Differing Spatial Features of Calcium Transients during Early and Delayed Afterdepolarizations in Guinea Pig Ventricular Myocytes

博 士 論 文

Differing Spatial Features of Calcium Transients during Early and Delayed Afterdepolarizations in Guinea-Pig Ventricular Myocytes

モルモット心室筋細胞における早期，遅延後電位時の細胞内カルシウムイオン動態

東北大学大学院医学研究科 内科系専攻
（老人科学講座）

三　浦　昌　人

博士論文

Differing Spatial Features of Calcium Transients during Early and Delayed Afterdepolarizations in Guinea-Pig Ventricular Myocytes

モルモット心室筋細胞における早期、遅延後電位時の細胞内カルシウムイオン動態

東北大学大学院医学研究科内科系専攻（老人科学講座）

三浦昌人

[Abstract]

Although changes in intracellular Ca^{2+} concentration ($[Ca^{2+}]_i$) are spatially heterogeneous during spontaneous contraction in mammalian cardiac muscle, it has not yet been observed how $[Ca^{2+}]_i$ changes spatially within cardiac myocytes during delayed (DADs) and early afterdepolarizations (EADs). The aim of this study is to characterize the spatial features of the increase in $[Ca^{2+}]_i$ during such afterdepolarizations and to understand the ionic mechanisms responsible for them. Myocytes were enzymatically isolated from guinea-pig ventricles and loaded with fura-2 AM, the Ca^{2+} fluorescence indicator dye. Membrane potential was recorded with a conventional microelectrode technique, and spatiotemporal changes in fura-2 fluorescence and cell length were recorded using a digital TV system. After perfusion with potassium-free Tyrode solution, DADs and EADs were induced. During DADs fluorescence transients were heterogeneous within myocytes (n=11). Further, they often propagated within myocytes as if they were 'waves'. In contrast, during EADs fluorescence transients showed no 'waves' within myocytes but rather showed synchronous changes throughout the myocytes (n=15). The results of this study suggest that the spatial features of the increase in $[Ca^{2+}]_i$ differ between the DADs and EADs. We concluded from these differing features that the ionic mechanisms responsible for the two triggered activities are different.

[Introduction]

Increases in intracellular Ca^{2+} concentration ($[Ca^{2+}]_i$) during aftercontractions have been observed in multicellular preparations [1], and increases in $[Ca^{2+}]_i$ during the transient inward currents have been observed over the entire rat ventricular myocyte [4]. Recently, increases in $[Ca^{2+}]_i$ during early afterdepolarizations were also reported over the entire canine ventricular myocyte [38]. Although spatial heterogeneity of $[Ca^{2+}]_i$ during spontaneous contractions has been observed in mammalian cardiac muscle with the use of auquorin [32, 43] and Ca^{2+} fluorescence indicator dyes such as fura-2 [42] and indo-1 [40], the spatial changes in $[Ca^{2+}]_i$ within cardiac myocytes have not been observed at the same that delayed (DADs) and early afterdepolarizations (EADs) were occurring.

The primary factor initiating DADs is thought to be an elevation of $[Ca^{2+}]_i$ [15, 20, 26]. However, the relation between EADs and $[Ca^{2+}]_i$ has not yet been clearly established [29, 39], although recent studies suggest that the EADs are ascribable to an inward Ca^{2+} current that is carried through L-type Ca^{2+} channels [24]. In both cases, especially that of EADs, it is important to observe the spatial and temporal changes in $[Ca^{2+}]_i$ within cardiac myocytes. We therefore attempted to characterize the spatial features of the increase in $[Ca^{2+}]_i$ during such afterdepolarizations and to discover the ionic mechanisms responsible for them.

In this study we prepared isolated guinea pig ventricular myocytes and simultaneously recorded cell length, membrane potential and dynamic changes in fura-2 fluorescence inside the cells. We induced DADs [8, 37] and EADs [35] by perfusion with potassi-

um-free Tyrode solution and analyzed the spatial and temporal changes in fura-2 fluorescence signals within the myocytes during the afterdepolarizations.

[Methods]

1) Cell isolation and dye loading

Single myocytes were prepared by a modification of a technique previously described by Taniguchi et al. [41]. In brief, guinea-pigs (250-300 g) were lightly anesthetized with diethyl ether. Hearts were excised and the coronary artery was perfused through the cut end of the aorta (Langendorff perfusion) with Tyrode solution (normal Tyrode) containing in mM: NaCl 136.9, KCl 5.4, $CaCl_2$ 1.8, $MgCl_2$ 0.53, NaH_2PO_4 0.33, HEPES 5.0 and glucose 10. pH was adjusted to 7.4 by adding NaOH. After the blood was washed out, the perfusate was replaced by nominally calcium-free Tyrode. The relaxed heart was then perfused with the nominally Ca-free Tyrode containing 0.05 mg/ml collagenase (Yakult) for 8 min. After the enzyme treatment, the heart was washed with 100 ml of a high K^+, low Cl^- solution (KB solution) containing in mM: taurine 10, oxalic acid 10, glutamic acid 70, KCl 25, KH_2PO_4 10, HEPES 10, glucose 11 and EGTA 0.5. pH was adjusted to 7.4 by adding KOH. The softened hearts were cut into several pieces and incubated in Erlenmeyer flasks containing 20 ml of KB solution. The dispersed myocytes were filtered through nylon mesh and centrifuged at 37 X g for 1 min. The sedimented myocytes were suspended in KB solution, stored for 10 min and centrifuged at 37 X g for 1 min. The myocytes were then suspended in the normal Tyrode with 1.8 mM $CaCl_2$. This isolation procedure was carried

out at 37° C.

The myocytes were then loaded with fura-2 by exposure to the acetoxymethyl ester of fura-2, fura-2 AM (Dojin Chemical), at a concentration of 2 μM for 30 min. After loading, extracellular fura-2 AM was washed out by centrifugation at 37 X g for 1 min, and the myocytes were suspended in fresh normal Tyrode. This loading procedure was carried out at room temperature. All solutions used in this experiment were gassed with 100 % O_2.

2) Recording of fluorescence images

Fluorescence images of myocytes were recorded as previously reported [22, 23]. Briefly, a small number of the fura-2 loaded myocytes were placed in an experimental chamber mounted on the stage of an inverted microscope (Nikon, TMD) equipped with an epifluorescence illuminator, an ultrasensitive video camera and a digital image processing unit (Fig. 1). We used a single wavelength at 380 nm as an excitation source because we were interested in dynamic changes in the regional $[Ca^{2+}]_i$ rather than the absolute value of the $[Ca^{2+}]_i$. Fluorescence from a fura-2 loaded myocyte was recorded using a x40 objective lens (Nikon Fluor 40, N.A.=0.85, working distance = 0.23 mm), filtered at 510 nm and projected onto a silicon intensifier target (SIT) video camera (Hamamatsu c2400-8). The video signal from the camera was recorded with a video recorder (National, AG-6300) for later analysis. The video data of one frame was digitalized and stored in a frame buffer memory of 256 x 256 pixels (Photoron, FDM-98). In this recording apparatus, the framing rate of the video system, 30 frame/sec, limited the time resolution of the measurements. In

addition, the SIT camera used here showed a "lag" and a "persistence" of output, which were evaluated as reported previously [23]. These limitations may have slightly distorted the recording of actual Ca^{2+} transients at their peaks and tails. However, we were concerned here only with the existence and propagation of the regional Ca^{2+} transients rather than with the details of the wave form.

3) Recording of membrane potential

For measurement of membrane potential we used a conventional microelectrode technique (Fig. 1). Myocytes were impaled with 3 M KCl-filled microelectrodes (30-50 MΩ). Microelectrodes were connected to an oscilloscope (Iwatsu Electric Co., LTD, SS-5100 Synchroscope) and chart recorder (Graphtec WR3701) through a microelectrode amplifier with a high input impedance (Nihon Kohden, MEZ-8201). Action potentials were evoked by brief current pulses through the recording microelectrode.

4) In vitro calibration for fura-2 fluorescence

In order to evaluate the responsiveness of our system for Ca^{2+} measurement, an in vitro calibration for fura-2 fluorescence was performed on the same apparatus used for the experiments (Fig. 1, inset). The calibration solution contained 147 mM KCl, 1 mM $MgCl_2$, 1 mM EGTA, 10 mM HEPES, 10 mM NaHEPES and 70 μM fura-2. We added $CaCl_2$ to the solution and adjusted the Ca^{2+} concentration by the Ca^{2+} electrode from 10^{-8} M to 10^{-3} M. Each calibration solution was perfused into a space between two cover-glasses aligned in parallel at a distance of 150 μm and illuminated with 340 nm and 380 nm light in turn. The inset of Fig. 1 shows light intensities during illumination with 340 nm and 380 nm light

plotted as a function of Ca^{2+} concentration. With an increase in Ca^{2+} concentration the light intensity during illumination with 340 nm light increased, and the intensity during illumination with 380 nm light decreased. Within the range of reported Ca^{2+} concentration during contraction in cardiac muscles [30], i.e., from 100 nM (pCa 7) to 10 μM (pCa 5), the change in fluorescence intensities during illumination with 380 nm light reflected more clearly the change in Ca^{2+} concentration. Thus, in this study the change in fluorescence during illumination with 380 nm was used as an indicator of relative change in $[Ca^{2+}]_i$.

5) Analysis of images

For analysis of the fluorescence images of myocytes, intensity profiles of the fluorescence were obtained, as previously reported [23]. A sampling line was set along the long axis of the myocyte, and the intensity value at a given pixel on the sampling line was calculated as the mean value of a 5 X 5 pixel (5 X 5 μm) area centered on that pixel. Since the intensity of the fluorescence is a function of position and time, we required a three dimensional display. In this paper all figures are shown on time-position plots that were constructed by stacking up the temporal changes in light intensity at the pixel positions along the sampling line. In these figures, each intensity profile was subtracted from the control which was recorded in the absence of cell contraction, and the temporal differences in light intensity were displayed so that an upward deflection indicates fluorescence changes corresponding to an increase in $[Ca^{2+}]_i$ (- delta light intensity).

The change in cell length was measured by the motions of both cell edges in serial fluorescence images of myocytes. We showed the change as a ratio to the resting length of the myocyte. The amount of shortening varied cell by cell depending on the contractility of the myocyte and the degree of attachment to the bottom of the experimental chamber.

6) Experimental protocol

In this study we selected rod shaped, clearly striated myocytes that were well loaded with fura-2 and exhibited no spontaneous contractions. After a successful impalement with the microelectrode, the myocyte was superfused with potassium-free Tyrode, which was made simply by omitting KCl from the normal Tyrode. A few minutes after the superfusion, DADs and EADs were induced. In this study, we defined DADs as depolarizations which occurred after full repolarization and EADs as depolarizations which occurred during the plateau (second phase of an action potential). Myocytes that showed lateral motion or swing were discarded. We analyzed data from myocytes whose amount of shortening during DADs and EADs was less than 10 % even if the amount of shortening during twitch contractions was more than 10 %, because our purpose of this study was to characterize the spatial features of increase in $[Ca^{2+}]_i$ during DADs and EADs. As previously reported [22, 23], motion artifacts resulting from increased cell thickness during shortening would be negligible when the amount of shortening was less than 10 %. In this study, we analyzed eleven DADs in seven myocytes and fifteen EADs in five myocytes. All experiments reported here were carried out at a temperature of 30° C.

[Result]

In Fig. 2 we display an example of a DAD. The upper panel shows membrane potential, the middle panel shows spatial and temporal changes in fura-2 fluorescence processed by the subtraction procedure (described in METHODS) and the lower panel shows cell length. In the upper panel a DAD can be observed (shown by an arrow) after an action potential was evoked by a brief current pulse through the recording microelectrode. By the action potential, fura-2 fluorescence transients were elicited synchronously throughout the myocyte, as shown in the middle panel. After the synchronous fluorescence transients, focal fluorescence transients emerged spontaneously at the center of the myocyte and spread in both directions. The propagating pattern of the fluorescence transients seemed to be wavelike. Here, it should be noted that the spontaneous fluorescence transients are occurring concomitant with the DAD (upper panel) and a spontaneous contraction (lower panel). During all eleven analyzed DADs in seven myocytes, the fluorescence transients were consistently heterogeneous within myocytes and often showed a wavelike pattern, as shown in Fig. 2.

In contrast, the spatial features of fluorescence transients during EADs were different from those during DADs. In Fig. 3 we display an example of an EAD. In the upper panel an EAD was occurring proceeding from the plateau phase (second phase) of an action potential evoked by a brief current pulse (shown by an arrow). In the middle panel, synchronous fluorescence transients were elicited throughout the myocyte by the action potential.

Proceeding from the fluorescence transients, we found synchronous changes in fluorescence signals throughout the myocyte, which were concomitant with the EAD (upper panel) and the sustained contraction (lower panel).

About one minute after further perfusion of potassium-free Tyrode, repetitive EADs were observed in the myocyte (Fig. 4). In the upper panel EADs appeared repeatedly proceeding from the plateau phase of the action potential. During such EADs the change in fluorescence signals was sustained, proceeding from the fluorescence transients elicited by the action potential, as shown in the middle panel. Furthermore, it should be noted that the fluorescence transients showed no 'waves' but rather showed synchronous changes throughout the myocytes. Here, we can observe some small fluctuations in the fluorescence signals during the EADs. It seems, however, more probable that such fluctuations resulted not from the fluctuations in $[Ca^{2+}]_i$ but from some measuring noise, because it is difficult to distinguish the fluctuations during the EADs and from those during resting membrane potential. In the lower panel the shortening of cell length continued until the EADs ceased. Such synchronous changes of the fluorescence transients during EADs could be observed consistently during all fifteen analyzed EADs in five myocytes.

[Discussion]

It is generally accepted that in mammalian cardiac muscle there is an increase in $[Ca^{2+}]_i$ during aftercontractions [1] or during the transient inward current [4]. Recently, an increase in $[Ca^{2+}]_i$ was also observed during EADs [38]. Thus, when we char-

acterize the roles of Ca^{2+} in the occurrence of such afterdepolarizations, it is necessary to observe the spatial patterns of increase in $[Ca^{2+}]_i$ within myocytes during the afterdepolarizations. As described above, during DADs fluorescence transients showed heterogeneous changes and often propagated within myocytes as if they were 'waves' (Fig. 2). In contrast, during EADs fluorescence transients showed synchronous changes throughout myocytes (Fig. 3 and 4).

Recently, heterogeneous fluorescence transients were observed during spontaneous contractions [4, 22, 23, 40], and have been attributed to Ca^{2+} induced Ca^{2+} release from the sarcoplasmic reticulum (SR) [17, 27, 32, 43]. These spontaneous contractions do not require an intact sarcolemma as indicated on the fact that they occur in myocytes that are devoid of sarcolemma [17]. Thus, the heterogeneous fluorescence transients observed during DADs in this study also may be mediated by Ca^{2+} induced Ca^{2+} release from the SR, which supports the concept that during DADs an increase in $[Ca^{2+}]_i$ primarily occurs and consequently leads to an increased inward current [25, 31] arising from Na^+-Ca^{2+} exchangers [2, 19] and non-specific cation channels [7, 9, 14, 26].

During the second phase of the action potential from which EADs arose in this study, various inward and outward currents are concerned. The inward currents include a time-independent Na^+ "window" current [3], a time-dependent Na^+ current through slowly inactivating Na^+ channels [10], and Ca^{2+} current through L-type Ca^{2+} channels. The outward currents prominently include two K^+ currents, the delayed rectifier (i_k) [18] and the inward rectifier (i_{k1}) [36]. The other currents not carried by ionic channel in-

clude the outward current generated by the Na^+-K^+ exchange membrane pump and the inward current generated by electrogenic Na^+-Ca^{2+} exchange. It has been established that EADs can be induced by the following interventions which increase the inward currents and those which reduce the outward currents. The perfusion of aconitine [33], anthopleurin-A [16], and Bay K 8644 [24] can induce EADs by increasing inward currents. The perfusion of low K [35], Cs^+ [6, 12, 28], and quinidine [13] can induce EADs by reducing outward currents. Low frequency of stimulation can also reduce the outward current through a decrease in the rate of Na^+-K^+ exchange. Despite an increasing number of interventions which can induce EADs, precise ionic mechanisms underlying EADs are still controversial, and following mechanisms have been proposed: 1) Na^+ "window" current [6, 34], 2) Ca^{2+} "window" current [21, 24], 3) the transient inward current activated by $[Ca^{2+}]_i$ [39], and 4) reduced outward K^+ current. In this study, we perfused myocytes with potassium-free Tyrode. It may cause the decreases in both inwardly rectifying K^+ conductance and the rate of Na^+-K^+ exchange, leading to a reduction of net outward current. Such the reduction of net outward current can prolong the second phase of the action potential and may provide a conditioning phase required for the induction of EADs.

As noted previously, forced mobilization of Ca^{2+} from intracellular stores is a primary cause for the genesis of DADs. A contribution of Ca^{2+} for the genesis of EADs are less understood. Szabo et al. reported in a preliminary form that EADs in Cs^+ treated canine ventricular myocyte accompanied sustained increase

in $[Ca^{2+}]_i$ [39]. They observed $[Ca^{2+}]_i$ over a entire isolated cell and did not concern with the spatial feature of $[Ca^{2+}]_i$ inside the myocyte. There might be a possibility that the mobilization of Ca^{2+} can contribute to the genesis of EADs in a similar way for the genesis of DADs via the transient inward current activated by $[Ca^{2+}]_i$. Our observation in this study on the spatial feature, however, showed synchronous changes in the fluorescence transients during EADs. Thus, we can eliminate the primary contribution of Ca^{2+} mobilization for the genesis of EADs.

While the direct aim of this study is not to determine the mechanism responsible for EADs, our results give some clues to know which mechanism is most probable. If we did not take account of the Ca^{2+} "window" current, i.e., a current caused by partial inactivation and sustained partial activation [21], Ca^{2+} inward current through L-type Ca^{2+} channel would become inactivated at the second phase of the action potential. On the other hand, Ca^{2+} release mechanism from the SR showed refractoriness because of either an inactivation of Ca^{2+} release channel or a depletion of releasable Ca^{2+} inside the SR (23). In this case, to sustain the increase in $[Ca^{2+}]_i$, Ca^{2+} must be supplied from extracellular space or Ca^{2+} store site other than the SR, i.e., mitochondria. Since it has been generally considered that Ca^{2+} mobilization from mitochondria does not depend on transsarcolemmal voltage, Ca^{2+} entry across sarcolemma is necessary. Re-activation of L-type Ca^{2+} channel might be also responsible, but EADs that we concern in this study arose from the plateau level (-10 to -30 mV) at which L-type Ca^{2+} channel can not be recovered. Such the re-activation of L-type Ca^{2+} channel may contribute to the Ca^{2+}

entry during EADs arising from around -60 mV at which Na^+ window current is most active [11]. Another possible route of Ca^{2+} entry is Na^+-Ca^{2+} exchange. But, recent experimental result in intact rabbit ventricular muscle shows that Ca^{2+} entry via Na^+-Ca^{2+} exchange does not normally contribute significantly to an increase in $[Ca^{2+}]_i$ [5]. Thus, it seems difficult to explain the sustained and synchronous change in fluorescence transients observed in this study without taking account of Ca^{2+} "window" current.

The results in this study suggest that the spatial features of the increase in $[Ca^{2+}]_i$ differ between the DADs and EADs. We conclude from these differing features that the ionic mechanisms responsible for the two triggered activities may be different.

[Reference]

1. Allen, D.G., D.A. Eisner, J.S Pirolo, and G.L. Smith. The relationship between intracellular calcium and contraction in calcium-overloaded ferret papillary muscles. J. Physiol. Lond. 364: 169-182, 1985.

2. Arlock, P., and B.G. Katzung. Effects of sodium substitutes on transient inward current and tension in guinea-pig and ferret papillary muscle. J. Physiol. Lond. 360: 105-120, 1985

3. Attwell, D., I. Cohen, D. Eisner, M. Ohba, and C. Ojeda. The steady state TTX-sensitive ("window") sodium current in cardiac Purkinje fibers. Pflugers Arch. 379: 137-142, 1979.

4. Berlin, J.R., M.B. Cannell, and W.J. Lederer. Cellular origins of the transient inward current in cardiac myocytes. Role of fluctuations and waves of elevated intracellular calcium. Circ. Res. 65: 115-126, 1989.

5. Bers, D.M., D.M. Christensen, and T.X. Nguyen. Can Ca entry via Na-Ca exchange directly activate cardiac muscle contraction ? J. Mol. Cell. Cardiol. 20: 405-414, 1988.

6. Brachmann, J., B.J. Scherlag, L.V. Rosenshtraukh, and R. Lazzara. Bradycardia-dependent triggered activity: relevance to drug-induced multiform ventricular tachycardia. Circulation 68: 846-856, 1983.

7. Cannell, M.B., and W.J. Lederer. The arrhythmogenic current I_{TI} in the absence of electrogenic sodium-calcium exchange in sheep cardiac Purkinje fibers. J. Physiol. Lond. 374: 201-219, 1986.

8. Cannell, M.B., R.D. Vaughan-Jones, and W.J. Lederer. Ryanodine

block of calcium oscillations in heart muscle and the sodium-tension relationship. Federation Proc. 44: 2964-2969, 1985.

9. Colquhoun, D., E. Neher, H. Reuter, and C.F. Stevens. Inward current channels activated by intracellular Ca in cultured cardiac cells. Nature Lond. 294: 752-754, 1981.

10. Carmeliet, E. Slow inactivation of the sodium current in rabbit cardiac Purkinje fibers. Pflugers Arch. 408: 18-26, 1987.

11. Coulombe, A., E. Coraboeuf, and C. Malecot. Role of the "Na window" and other ionic currents in triggering early afterdepolarizations and resulting reexcitations in Purkinje fibers. Cardiac electrophysiology and arrhythmias. Edited by D.P. Zipes, J. Jalife. New York, Grune & Stratton: 43-49, 1985.

12. Damiano, B.P., and M.R. Rosen. Effects of pacing on triggered activity induced by early afterdepolarizations. Circulation 69: 1013-1025, 1984.

13. Davidenko, J.M., L. Cohen, R. Goodrow, and C. Antzelevitch. Quinidine-induced action potential prolongation, early afterdepolarizations, and triggered activity in canine Purkinje fibers: Effects of stimulation rate, potassium, and magnesium. Circulation 79: 674-686, 1989.

14. Ehara, T., A. Noma, and K. Ono. Calcium-activated non-selective cation channel in ventricular cells isolated from adult guinea-pig hearts. J. Physiol. Lond. 403: 117-133, 1988.

15. Eisner, D.A. The role of intracellular Ca ions in the therapeutic and toxic effects of cardiac glycosides and catecholamines. J. Cardiovasc. Pharmacol. 8(Suppl3): S2-S9, 1986.

16. El-Sherif, N., R.H. Zeiler, W. Craelius, W.B. Gough, and R. Henkin. QTU prolongation and polymorphic ventricular tachyar-

rhythmias due to bradycardia-dependent early afterdepolarizations: Afterdepolarizations and ventricular arrhythmias. Circ. Res. 63: 286-305, 1988.

17. Fabiato, A., and F. Fabiato. Contractions induced by a calcium-triggered release of calcium from the sarcoplasmic reticulum of single skinned cardiac cells. J. Physiol. Lond. 249: 469-495, 1975.

18. Fan, Z., and M. Hiraoka. Depression of delayed outward K^+ current by Co^{2+} in guinea pig ventricular myocytes. Am. J. Physiol. 261 (Cell Physiol. 30): C23-C31, 1991.

19. Fedida, D., D. Noble, A.C. Rankin, and A.J. Spindler. The arrhythmogenic transient inward current i_{TI} and related contraction in isolated guinea-pig ventricular myocytes. J. Physiol. Lond. 392: 523-542, 1987.

20. Ferrier, G.R. Digitalis arrhythmias: Role of oscillatory afterpotentials. Progr. Cardiovasc. Dis. 19: 459-474, 1977.

21. Hirano, Y., A. Moscucci, and C.T. January. Direct Measurement of L- type Ca^{2+} window current in heart cells. Circ. Res. 70: 445-455, 1992.

22. Ishide, N., M. Miura, M. Sakurai, and T. Takishima. Initiation and development of calcium waves in rat myocytes. Am. J. Physiol. 263 (Heart Circ. Physiol. 32): H327-H332, 1992.

23. Ishide, N., T. Urayama, K. Inoue, T. Komaru, and T. Takishima. Propagation and collision characteristics of calcium waves in rat myocytes. Am. J. Physiol. 259 (Heart Circ. Physiol. 28): H940-H950, 1990.

24. January, C.T., and J.M. Riddle. Early afterdepolarizations:

Mechanism of induction and block. A role for L-type Ca^{2+} current. Circ. Res. 64: 977-990, 1989.

25. Kass, R.S. Fluctuations in membrane current driven by intracellular calcium in cardiac Purkinje fibers. Biophys. J. 38: 259-269, 1982.

26. Kass, R.S., W.J. Lederer, R.W. Tsien, and R. Weingart. Role of calcium ions in transient inward currents and aftercontractions induced by strophanthidin in cardiac Purkinje fibers. J. Physiol. Lond. 281: 187-208, 1978.

27. Lakatta, E.G., M.C. Capogrossi, A.A. Kort, and M.D. Stern. Spontaneous myocardial calcium oscillations: Overview with emphasis on ryanodine and caffeine. Federation Proc. 44: 2977-2983, 1985.

28. Levine, J.H., J.F. Spear, T. Guarnieri, M.L. Weisfeldt, C.D.J. De Langen, L.C. Becker, and E.N. Moore. Cesium chloride-induced long QT syndrome: demonstration of afterdepolarizations and triggered activity in vivo. Circulation 72: 1092-1103, 1985.

29. Marban, E., S.W. Robinson, and W.G. Wier. Mechanisms of arrhythmogenic delayed and early afterdepolarizations in ferret ventricular muscle. J. Clin. Invest. 78: 1185-1192, 1986.

30. Marban, E., T.J. Rink, R.W. Tsien, and R.Y. Tsien. Free calcium in heart muscle at rest and during contraction measured with Ca^{2+}-sensitive microelectrodes. Nature Lond. 286: 845-850, 1980.

31. Matsuda, H., A. Noma, Y. Kurachi, and H. Irisawa. Transient depolarization and spontaneous voltage fluctuations in isolated single cells from guinea pig ventricles. Calcium-mediated membrane potential fluctuations. Circ. Res. 51: 142-151, 1982.

32. Orchard, C.H., D.A. Eisner, and D.G. Allen. Oscillations of intracellular Ca^{2+} in mammalian cardiac muscle. Nature Lond. 304: 735-738, 1983.

33. Peper, K., and W. Trautwein. The effect of aconitine on the membrane current in cardiac muscle. Pflugers Arch. 296: 328-336, 1967.

34. Quantz, M.A., and S. Nattel. The ionic mechanism for quinidine-induced early afterdepolarizations. Circulation 74(Supple II): II-402, 1986.

35. Roden, D.M., and D.H.S. Iansmith. Effects of low potassium or magnesium concentrations on isolated cardiac tissue. Am. J. Med. 82(Supple 3A): 18-23, 1987.

36. Shimoni, Y., R.B. Clark, and W.R. Giles. Role of an inwardly rectifying potassium current in rabbit ventricular action potential. J. Physiol. 448: 709-727, 1992.

37. Sutko, J.L., and J.L. Kenyon. Ryanodine modification of cardiac muscle responses to potassium-free solutions. Evidence for inhibition of sarcoplasmic reticulum calcium release. J. Gen. Physiol. 82: 385-404, 1983.

38. Szabo, B., R. Sweidan, R. Fugate, T. Banyasz, and R. Lazzara. Ca^{2+} transients during generation of early afterdepolarizations in Cs^{+} treated canine ventricular myocytes. Circulation 82(Suppl III): III-746, 1990.

39. Szabo, B., R. Sweidan, E. Patterson, B.J. Scherlag, and R. Lazzara. Increased intracellular Ca^{2+} may be important also for early afterdepolarizations. J. Am. Coll. Cardiol. 9: 210A, 1987.

40. Takamatsu, T., and W.G. Wier. Calcium waves in mammalian

heart: quantification of origin, magnitude, waveform, and velocity. FASEB J. 4: 1519-1525, 1990.

41. Taniguchi, J., S. Kokubun, A. Noma, and H. Irisawa. Spontaneously active cells isolated from the sino-atrial and atrio-ventricular nodes of the rabbit heart. Jpn. J. Physiol. 31: 547-558, 1981.

42. Wier, W.G., M.B. Cannell, J.R. Berlin, E. Marban, and W.J. Lederer. Cellular and subcellular heterogeneity of $[Ca^{2+}]_i$ in single heart cells revealed by fura-2. Science Wash. DC 235: 325-327, 1987.

43. Wier, W.G., A.A. Kort, M.D. Stern, E.G. Lakatta, and E. Marban. Cellular calcium fluctuations in mammalian heart: Direct evidence from noise analysis of aequorin signals in Purkinje fibers. Proc. Natl. Acad. Sci. USA 80: 7367-7371, 1983.

[Figure Legends]

Figure 1

Experimental setup. This simplified diagram shows the optics used for measurement of fluorescence signals and the electronics used for measurement of membrane potential. The inset shows an in vitro calibration for fura-2 fluorescence and depicts light intensities during illumination with 340 nm (closed triangle) and 380 nm light (closed square) plotted as a function of Ca^{2+} concentration. Ex340, excitation wavelength at 340 nm; Ex380, excitation wavelength at 380 nm; IF 340 nm, interference filter at 340 nm; IF 380 nm, interference filter at 380 nm; IF 510 nm, interference filter at 510 nm.

Figure 2

Spatial changes in fluorescence signals during a DAD. The upper panel shows membrane potential, the middle panel shows spatiotemporal changes in fura-2 fluorescence signals and the lower panel shows cell length. In the middle panel focal fluorescence transients emerged spontaneously at the center of the myocyte and spread in both directions after fluorescence transients were elicited by an action potential. The propagating patterns of the fluorescence transients seemed to be 'waves'. It should be noted that the spontaneous fluorescence transients were occurring concomitant with a DAD in the upper panel (shown by an arrow) and a spontaneous contraction in the lower panel. Ex380, excitation wavelength at 380 nm; ST, electrical stimulation.

Figure 3

Spatial changes in fluorescence signals during an EAD (upper panel, shown by an arrow), proceeding from the plateau phase of an action potential, During the EAD we found synchronous changes in fluorescence transients throughout the myocyte as shown in the middle panel. Ex380, excitation wavelength at 380 nm; ST, electrical stimulation.

Figure 4

Spatial changes in fluorescence signals during EADs. In the upper panel EADs appeared repeatedly proceeding from the plateau phase of the action potential. Note that during EADs the change in fluorescence signals was sustained throughout the myocyte (middle panel). Although the fluorescence signal showed some fluctuations, they showed synchronous changes throughout the myocytes concomitant with the EADs. Ex380, excitation wavelength at 380 nm; ST, electrical stimulation.

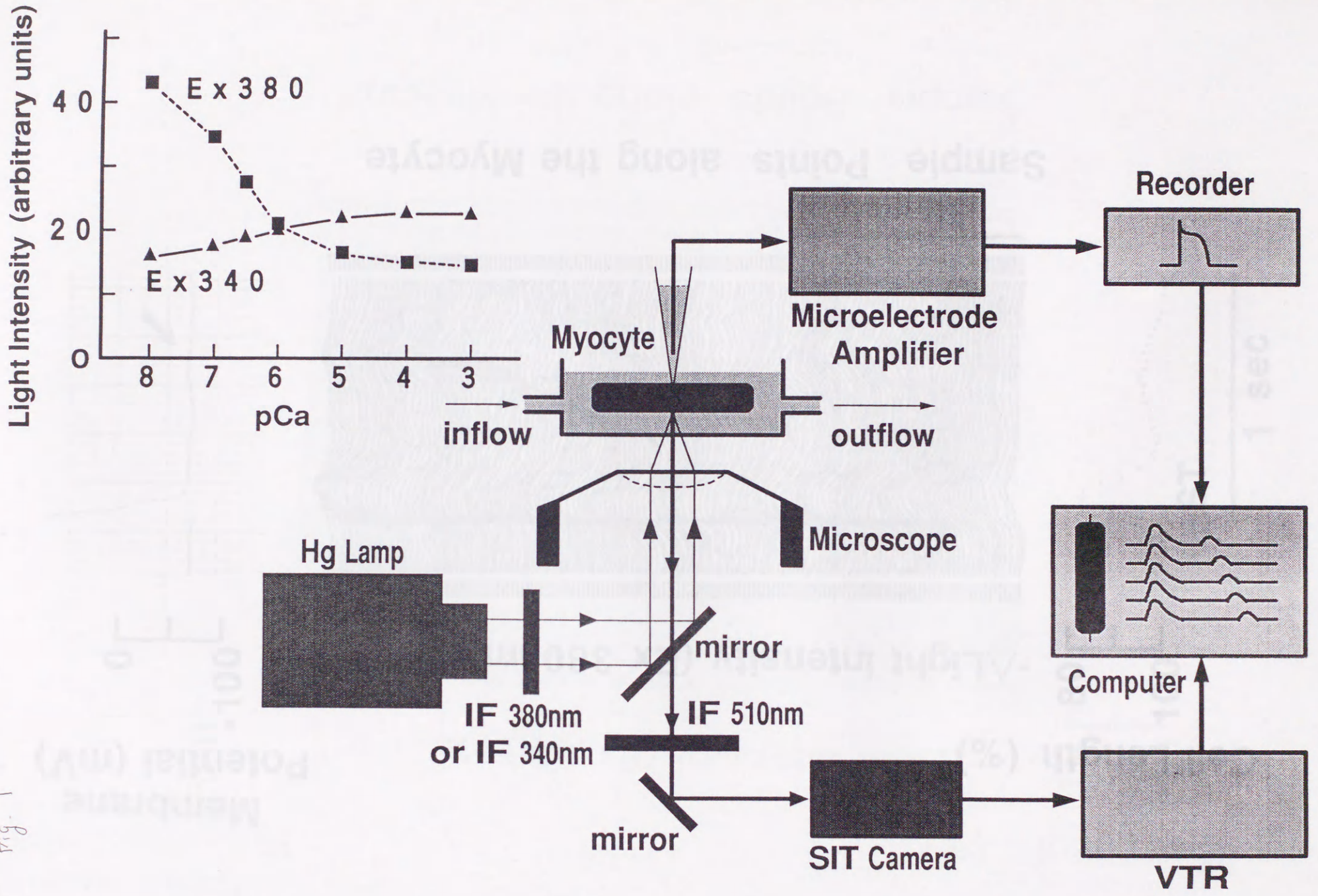
Light Intensity (arbitrary units)
40
20
0
Ex 380
Ex 340
8
7
6
5
4
3
pCa
Recorder
Microelectrode
Amplifier
Myocyte
inflow
outflow
Microscope
Hg Lamp
mirror
IF 380nm
or IF 340nm
IF 510nm
mirror
SIT Camera
Computer
VTR

Fig. 1

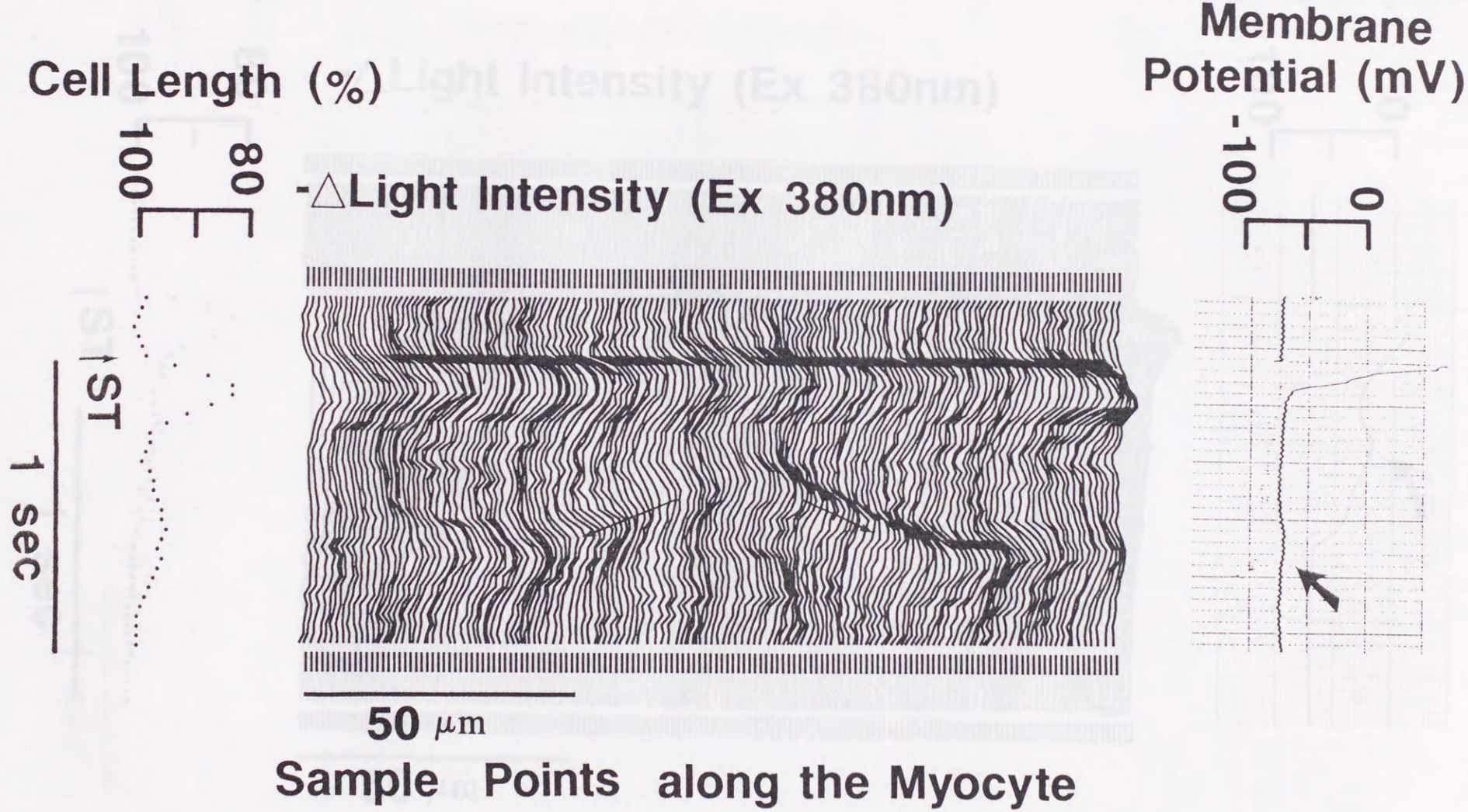
Cell Length (%)
100
80
-△Light Intensity (Ex 380nm)
Membrane Potential (mV)
-100
0
ST
1 sec
50 μm
Sample Points along the Myocyte

Fig-2

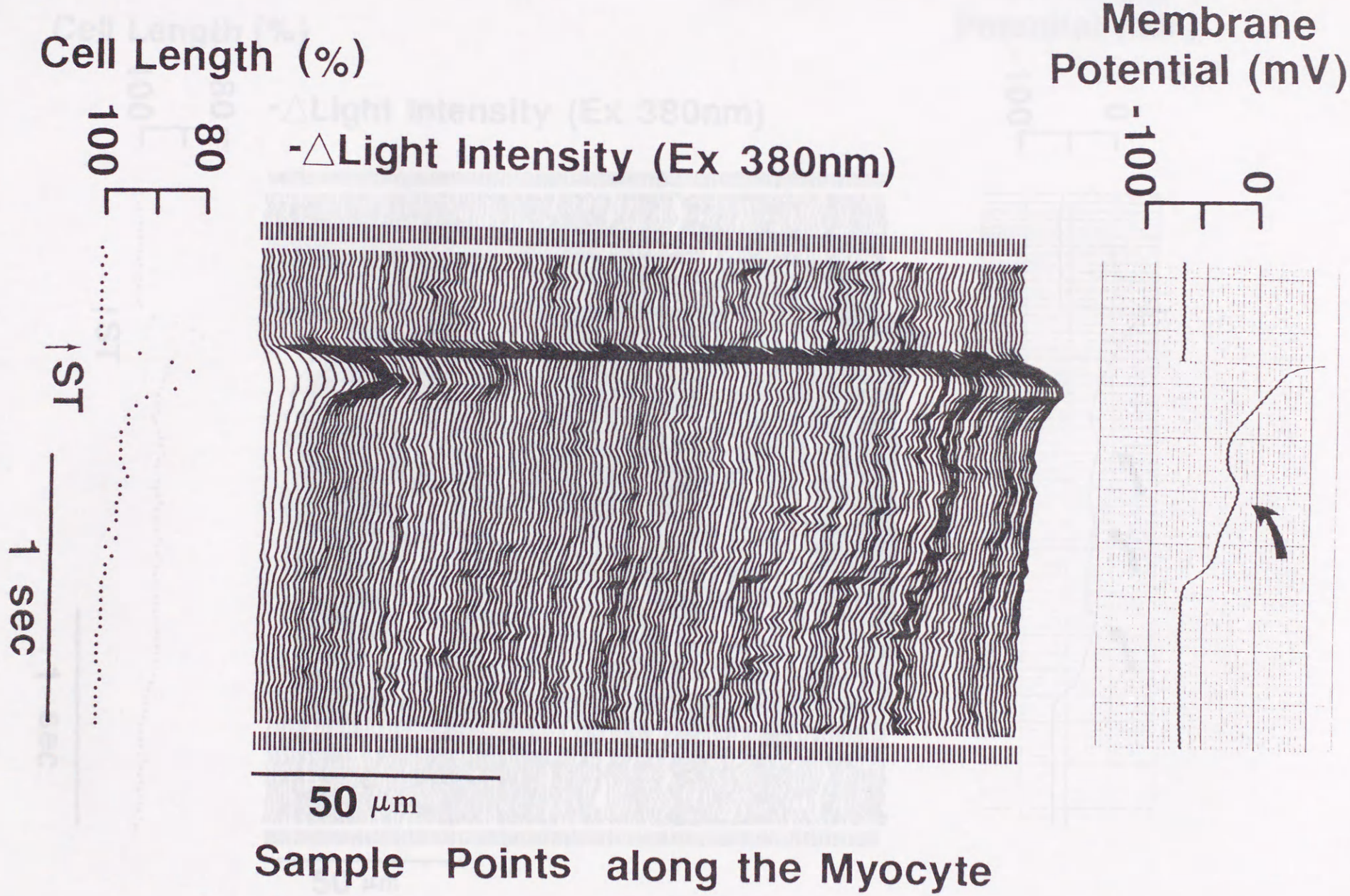
Cell Length (%)
100
80
ST
1 sec
-△Light Intensity (Ex 380nm)
50 μm
Membrane Potential (mV)
-100
0
Sample Points along the Myocyte

Fig. 3

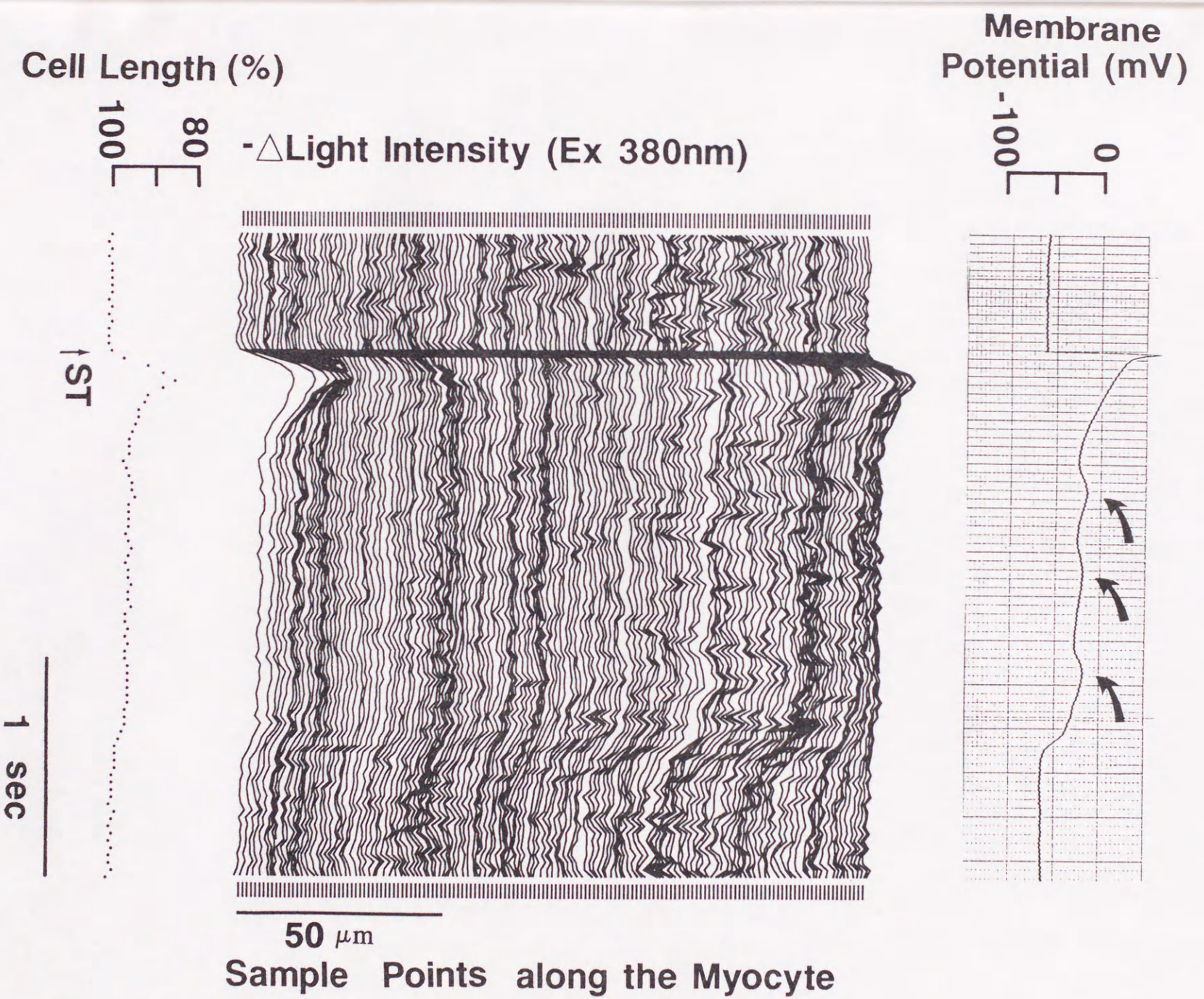
Cell Length (%)
100
80
-△Light Intensity (Ex 380nm)
Membrane Potential (mV)
-100
0
ST
1 sec
50 μm
Sample Points along the Myocyte

Fig. 4

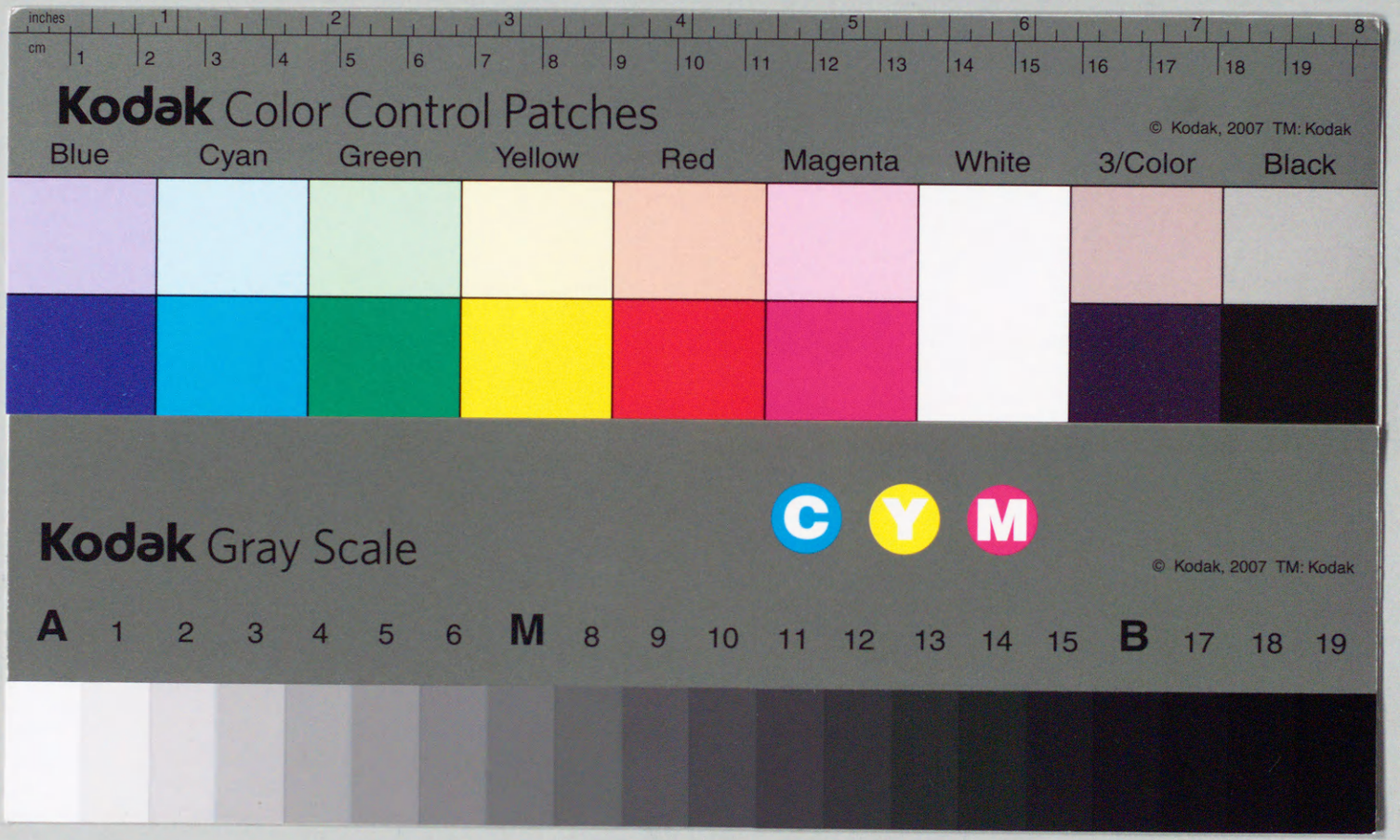
inches
cm
Kodak Color Control Patches
© Kodak, 2007 TM: Kodak
Blue
Cyan
Green
Yellow
Red
Magenta
White
3/Color
Black
Kodak Gray Scale
C
Y
M
© Kodak, 2007 TM: Kodak
A 1 2 3 4 5 6 M 8 9 10 11 12 13 14 15 B 17 18 19